

Chirally functionalized mesoporous organosilicas with built-in BINAP ligand for asymmetric catalysis†

Peiyuan Wang,^{ab} Xiao Liu,^{ab} Jie Yang,^a Yan Yang,^{ab} Lei Zhang,^a Qihua Yang^{*a} and Can Li^a

Received 10th July 2009, Accepted 25th August 2009

First published as an Advance Article on the web 21st September 2009

DOI: 10.1039/b913808k

The chirally functionalized periodic mesoporous organosilica (PMO) with C_2 -symmetric chiral building blocks, BINAP (2,2'-bis(diphenylphosphino)-1,1'-binaphthyl), in the pore wall was successfully synthesized for the first time using a successive co-condensation and post-synthesis modification method. Chiral BINAPO (2,2'-bis(diphenylphosphinooxide)-1,1'-binaphthyl) bridging mesoporous organosilica with highly ordered 2-D hexagonal structure was first synthesized by co-condensation of (*R*)-5,5'-bis(3-triethoxysilylpropyl-1-ureyl)-2,2'-bis(diphenylphosphinooxide)-1,1'-binaphthyl with tetramethoxysilane in the presence of block copolymer P123 as template under weakly acidic conditions. The BINAPO in the pore wall of PMO was reduced with trichlorosilane to generate BINAP using a post-synthesis modification method. The chiral PMO with built-in BINAP (coordination with $[\text{RuCl}_2(\text{benzene})_2]$) is an efficient solid catalyst for the asymmetric hydrogenation of β -keto esters with ee as high as 99%, which is among the highest ever reported for the chirally functionalized PMOs in asymmetric catalysis.

1. Introduction

Mesoporous materials with well-ordered pore structure, large surface area, uniform pore size distribution and tunable pore diameter have potential applications in the fields of catalysis, biotechnology, adsorption and separation.^{1–6} The periodic mesoporous organosilicas (PMOs) with bridging organic groups distributed uniformly in the framework represent a recent breakthrough in material science.^{7–12} The organic groups in the framework of PMOs not only modify the surface properties of the materials, but also endow the PMOs with novel bulk properties, such as improved hydrothermal and mechanical stabilities, extending the “pore surface chemistry” of the hybrid materials to the “pore wall chemistry”.^{13–16} The unique properties of the PMOs make them attractive in a range of applications, especially in catalysis. It has been demonstrated that the PMOs generally show higher catalytic activity than the pure mesoporous silica counterparts due to their enhanced surface hydrophobicity. They can efficiently catalyze many reactions, such as acid/base reactions, hydrogenation, selective oxidation, C–C coupling reaction and even asymmetric reactions.¹⁷

Chirally functionalized PMOs with a combination of a rigid nanoporous structure and homogeneously distributed chiral ligands in the pore wall may be potential chiral solids for asymmetric catalysis. The synthesis of chirally functionalized

PMOs has attracted much research attention because the development of high-performance chiral solid catalysts is of extreme importance and ongoing academic and industrial interest.^{18–21} Previous studies show that several chirally functionalized PMOs have been synthesized using 100% chiral organosilane compounds or mixtures of tetraethoxysilane (TEOS) and chiral organosilane as precursor under hydrothermal conditions.^{22–26} However, only limited numbers of chiral PMOs have been tested in the asymmetric catalysis and the reported enantioselectivity was usually lower than 40%.^{22,23,26} The low chiral inducibility of chirally functionalized PMOs may be partly due to the fact that there still is a lack of methods to incorporate some efficient but air/moisture sensitive chiral ligands in the pore wall of PMOs and partly due to the difficulties in construction of highly ordered porous structure using the silane precursor containing large and flexible organic groups. The synthesis of highly efficient chirally functionalized PMOs for asymmetric catalysis still remains a challenge.

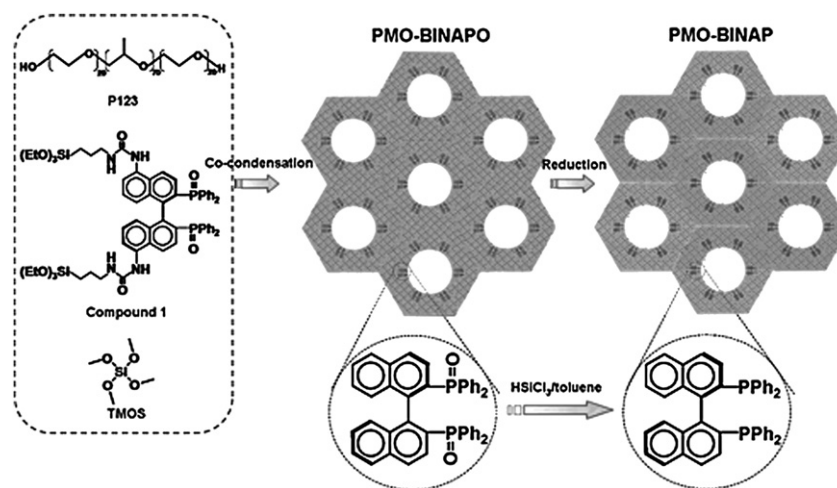
Among the various chiral blocks, the C_2 -symmetric bisphosphine ligand BINAP (2,2'-bis(diphenylphosphino)-1,1'-binaphthyl) reported by Noyori and Takaya in 1980 represents one of the most efficient chiral ligands. BINAP and its derivatives have been widely used in chiral synthesis and extensively investigated especially in asymmetric hydrogenation.^{27,28} The immobilization of BINAP has been a long-term research area in heterogeneous asymmetric catalysis. Though BINAP has been immobilized onto different kinds of supports, such as polymers, clays, silica, zirconium phosphonate, Fe_3O_4 , etc.,^{29–35} the incorporation of BINAP in the pore wall of PMOs has never been reported probably due to the instability of BINAP towards oxygen during the hydrothermal process.

Here we present the successful fusion of air sensitive BINAP in the pore wall of PMO by a successive co-condensation and post-synthesis modification method, as illustrated in Scheme 1. After

^aState Key Laboratory of Catalysis, Dalian Institute of Chemical Physics, Chinese Academy of Sciences, 457 Zhongshan Road, Dalian, 116023, China. E-mail: yangqh@dicp.ac.cn; Fax: +86 (0)411 84694447; Tel: +86 (0)411 84379552

^bGraduate School of the Chinese Academy of Sciences, Beijing, 100049, China

† Electronic supplementary information (ESI) available: FT-IR spectra of BINAP, $[\text{RuCl}_2(\text{benzene})_2]$ and Ru-BINAP. See DOI: 10.1039/b913808k



Scheme 1 Synthesis of chiral PMO with (*R*)-BINAP bridging in the pore wall.

coordination with $[\text{RuCl}_2(\text{benzene})]_2$, the chiral mesoporous materials can efficiently catalyze the asymmetric hydrogenation of β -keto esters with an ee as high as 99%.

2. Experimental

2.1. Materials

Poly(alkylene oxide) block copolymer (P123, $\text{EO}_{20}\text{PO}_{70}\text{EO}_{20}$) and $[\text{RuCl}_2(\text{benzene})]_2$ were purchased from Sigma-Aldrich Company, (USA). Trichlorosilane (HSiCl_3) was purchased from Alfa-Aesar, (USA). 2,2'-Bis(diphenylphosphino)-1,1'-binaphthyl ((*R*)-BINAP) was obtained from Shijiazhuang Shengjia Chemical Co, Ltd., (China). Tetramethoxysilane (TMOS) was obtained from Nanjing Shuguang Chemical Group (China). Other reagents were purchased from Shanghai Chemical Reagent Inc. of the Chinese Medicine Group. All solvents were of analytical quality and dried by standard methods.

2.2. Synthesis

The organosilane precursor, (*R*)-5,5'-bis(3-triethoxysilylpropyl-1-ureyl)-2,2'-bis(diphenylphosphino)-1,1'-binaphthyl (compound **1**) was synthesized from (*R*)-BINAP in multistep reactions according to a reported procedure.³⁶

BINAPO-containing chiral PMO, denoted as PMO-BINAPO, was synthesized by the co-condensation of compound **1** and TMOS with block copolymer P123 as a templating agent. 1.0 g of P123, 2.0 g of NaCl, and 0.30 mL of NH_4F solution (0.25 M) were mixed with 3.0 mL of HCl solution (0.1 M) and 27 mL of water. The solution was stirred at 40 °C for 3 h. Then, a mixture of TMOS (1.216 g), chiral silane **1** (1.179 g) and ethanol (4.00 g) was added to the above solution under vigorous stirring. The resultant mixture was further stirred at 40 °C for 20 h and then aged at 80 °C for 24 h. The molar ratio of Si : P123 : NaCl : NH_4F : H_2O : HCl : ethanol is 1 : 0.017 : 3.42 : 0.0075 : 166 : 0.03 : 8.7. As-synthesized material was extracted with ethanol under refluxing conditions for 24 h to remove the surfactant. After filtration, the powder was dried at 80 °C overnight.

BINAP-containing chiral PMO, denoted as PMO-BINAP, was synthesized from PMO-BINAPO. PMO-BINAPO was first

silylated by reaction with hexamethyldisilazane in hexane (1.0 g of PMO-BINAPO was refluxed in 25 mL of hexane and 1 mL of hexamethyldisilazane for 12 h). Under inert atmosphere, the silylated material was suspended in 20 mL of dry toluene containing 1.0 mL of HSiCl_3 . The mixture was heated to reflux for 40 h. HSiCl_3 (0.5 mL) was added to the mixture at 2, 7 and 18 h respectively. Using the Schlenk technique, the solid product was filtered and washed with CH_2Cl_2 . After drying under vacuum at room temperature, the obtained material was denoted as PMO-BINAP.

Coordination of PMO-BINAP with Ru complexes: PMO-BINAP (0.5 g) was placed in freshly distilled, degassed ethanol–benzene (10 mL (9 : 1)). To this mixture $[\text{RuCl}_2(\text{benzene})]_2$ (0.2 g, 0.8 mmol) was added and the resulting mixture was stirred at 60 °C for 24 h followed by hot filtration and several washing with methanol and CH_2Cl_2 . Elemental analysis of Ru is 0.412 mmol g^{-1} .

2.3. Asymmetric hydrogenation

Desired amounts of catalysts (Ru/PMO-BINAP), anhydrous methanol (1 mL) and substrates (110 μL , 1.0 mmol) were added in a test tube under argon. The test tube was transferred into a stainless steel autoclave and sealed. After purging with H_2 five times, the final H_2 pressure was adjusted to 4 MPa. After agitation at 50 °C for 24 h, H_2 pressure was released. The catalyst was separated with centrifugation and the organic solution was passed through a mini silica-gel column. The conversion of β -keto esters and enantiomeric excess of products were analyzed on an Agilent 6890 gas chromatograph equipped with a flame ionization detector and a Supelco γ -DEX 225 capillary column (30 m \times 0.25 mm \times 0.25 μm). For recycling the catalyst, all the liquids were collected carefully in vacuum after reaction. The residual catalyst was used directly for the next catalytic reaction.

2.4. Characterizations

X-Ray powder diffraction (XRD) patterns were recorded on a Rigaku RINT D/Max-2500 powder diffraction system using Cu $K\alpha$ radiation. The nitrogen sorption experiments were performed at –196 °C on an ASAP 2020 system. The samples were outgassed at 120 °C for 5 h before the measurements. The

Brunauer–Emmett–Teller (BET) surface area was evaluated from data in the relative pressure range of 0.05 to 0.25. The total pore volumes were estimated from the amount adsorbed at a relative pressure of 0.99. Pore diameters were determined from the adsorption branch using the Barrett–Joyner–Halenda (BJH) method. Transmission electron microscopy (TEM) was performed using a FEI Tecnai G² Spirit at an acceleration voltage of 120 kV. ¹³C (100.5 MHz) cross-polarization magic-angle spinning (CP-MAS), ³¹P (161.8 MHz), and ²⁹Si (79.4 MHz) MAS solid-state NMR experiments were recorded on a Varian infinity-plus 400 spectrometer equipped with a magic-angle spin probe in a 4-mm ZrO₂ rotor. ¹³C and ²⁹Si signals were referenced to tetramethylsilane, and ³¹P NMR signal was referenced to H₃PO₄ (85 wt %). The experimental parameters were 8-kHz spin rate, 3-s pulse delay, 4-min contact time, 1500–3000 scans for ¹³C CP-MAS NMR experiments; 4-kHz spin rate, 180-s pulse delay, 10-min contact time, 116 scans for ²⁹Si MAS NMR experiments; 10-kHz spin rate, 3-s pulse delay, 200 scans for ³¹P MAS NMR experiments.

3. Results and discussion

3.1. Synthesis and characterization of PMO-BINAPO

Due to the instability of BINAP towards oxygen during the hydrothermal process, compound **1**, (*R*)-5,5'-bis(3-triethoxysilylpropyl-1-ureyl)-2,2'-bis(diphenylphosphino-oxide)-1,1'-binaphthyl, was used as precursor for the synthesis. The XRD pattern of PMO-BINAPO is shown in Fig. 1A. Three well-resolved diffraction peaks were observed with *d* spacings of 9.8, 5.7 and 4.9 nm, which could be indexed to (100), (110) and (200) diffraction peaks of a highly ordered *P6mm* mesophase, respectively. The highly ordered pore structure of PMO-BINAPO was further confirmed by the TEM image (Fig. 2). A honeycomb structure as well as parallel fringe pore wall could be clearly observed in the TEM images of PMO-BINAPO with incidence direction parallel and perpendicular to the pore axis, respectively. The nitrogen sorption isotherm of PMO-BINAPO is of type IV with an H1 hysteresis loop in the relative pressure *P/P*₀ of 0.60 to 0.80, which is characteristic of mesoporous materials with large mesopores (Fig. 1B). PMO-BINAPO has pore diameter of

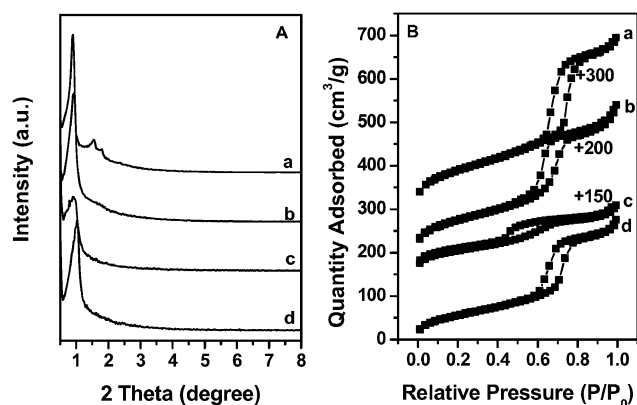


Fig. 1 XRD patterns (A) and nitrogen adsorption isotherms (B) of PMO-BINAPO (a), PMO-BINAPO (after silation) (b), PMO-BINAP (c) and Ru/PMO-BINAP (d).

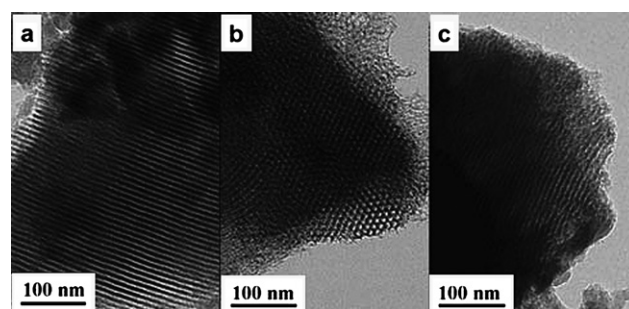


Fig. 2 TEM images of PMO-BINAPO (a, b) and PMO-BINAP (c).

7.7 nm, BET surface area of 331 m² g⁻¹ and a total pore volume of 0.61 cm³ g⁻¹ (Table 1). The above results show that PMO-BINAPO has highly ordered 2-D hexagonal mesostructure with large mesopore.

The FT-IR spectrum was employed for characterization of the chemical composition of PMO-BINAPO (Fig. 3). In the FT-IR spectrum of PMO-BINAPO, the ureylene stretching vibration is clearly observed at 1660 (overlapped with H₂O) and 1537 cm⁻¹ and the sharp peak at 1437 cm⁻¹ is ascribed to P–C (aryl) vibration of BINAPO ligand.³⁶ The peak at 3057 cm⁻¹ is ascribed to C–H (aryl) vibration of the BINAPO ligand. The vibrations of propyl group can be found at 2900 cm⁻¹. The vibration of P=O is overlapped with those of Si–O–Si in the range of 1000 to 1260 cm⁻¹. The absence of the C–H vibration peaks of P123 surfactant at 1375 cm⁻¹ suggests almost complete removal of the surfactant during the ethanol extraction process.³⁷

To further clarify the composition of PMO-BINAPO, ²⁹Si MAS NMR and ¹³C CP/MAS NMR were performed (Fig. 4). ²⁹Si MAS NMR spectrum of PMO-BINAPO shows both the T and Q silicon sites. The main signal at –112.3 ppm and the shoulder peak at –103.5 ppm correspond to Q⁴ [Si(OSi)₄] and Q³ [Si(OH)(OSi)₃] Si species, respectively. The broad peak centered at –66.7 ppm could be ascribed to the mixture of T³ [SiC(OSi)₃] and T² [SiC(OH)(OSi)₂] organosilicon species. The absence of T⁰ [SiC(OH)₃] site confirms that the chiral moiety is actually integrated with both ends in the pore walls, instead of dangling in the pore as a pendant group. The peak area ratio of $\Sigma T/(\Sigma T + \Sigma Q) \approx 20.4\%$, which agrees well with the silicon molar concentration of compound **1** in the initial mixture (20%), indicates that the weakly acidic synthesis conditions are efficient for stoichiometric incorporation of the organic groups in the mesoporous network. In the ¹³C CP/MAS NMR spectrum of PMO-BINAPO, signal at 154.5 ppm is from the carbonyl carbon (C=O). Signals in the range of 150–110 ppm can be ascribed to the aryl carbons of BINAPO. Signals at 42.8, 18.5 and 9.1 ppm are due to C³, C², and C¹ carbon species of Si–C¹H₂C²H₂C³H₂. The signals at 16.4 and 59.3 ppm may originate from the ethoxy groups formed during the surfactant-extraction process. No carbon species associated with the surfactant are observed, showing the efficiency of the ethanol extraction method. The amount of the chiral ligand PMO-BINAPO was 0.45 mmol g⁻¹ based on P elemental analysis. The results of structural and compositional characterization show that highly ordered chiral PMO with BINAPO ligands distributed in the framework can be obtained under hydrothermal conditions.

Table 1 Structural and textural properties of chiral PMOs

Sample	<i>d</i> spacing/nm	BET surface area/m ² g ⁻¹	Pore volume/cm ³ g ⁻¹	Pore diameter/nm ^a
PMO-BINAPO	9.8	331	0.61	7.7
PMO-BINAPO (after silylation)	9.4	280	0.53	6.6
PMO-BINAP	9.4	201	0.25	4.6
Ru/PMO-BINAP	8.5	211	0.42	7.1

^a Calculated using the BJH model on the adsorption branch of the isotherm.

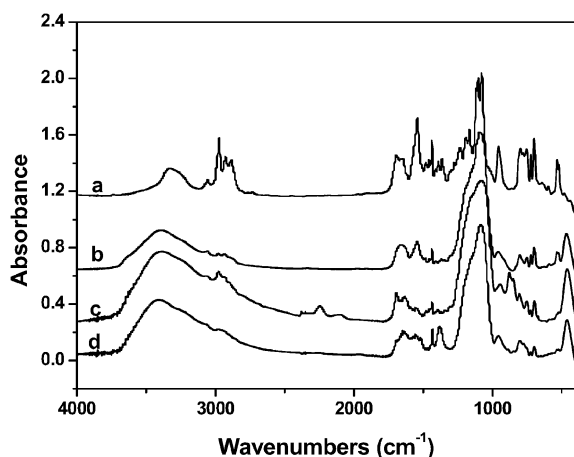


Fig. 3 FT-IR spectra of compound **1** (a), PMO-BINAPO (b), PMO-BINAP (c) and Ru/PMO-BINAP (d).

3.2. Synthesis and characterization of PMO-BINAP and Ru/PMO-BINAP

For application of the chiral PMO-BINAPO in asymmetric catalysis, it is desirable to reduce BINAPO into BINAP. The composition of PMO-BINAP after reduction was analyzed by ²⁹Si MAS NMR and ¹³C/CP MAS NMR (Fig. 4). Similar to PMO-BINAPO, both T and Q silicon sites were observed in the ²⁹Si MAS NMR spectrum of PMO-BINAP. Compared with PMO-BINAPO, the decrease in intensity of Q³ site [Si(OH)(OSi)₃] and upfield shift of T site indicate further framework condensation

during the post-synthesis modification process. The additional signal at 11.5 ppm is due to the silicon species connected with methyl group from the silylation process. The peak area ratio of ΣT/(ΣT + ΣQ) is ~18.9%, which is similar to that of PMO-BINAPO (~20.4%). This indicates that no Si–C bond cleavage occurred during the post-synthesis modification process.

In the ¹³C CP/MAS NMR spectrum of PMO-BINAP (Fig. 4), the chemical shifts of carbonyl carbon (C=O) and aryl carbons of BINAP and C², and C¹ carbon species of Si–C¹H₂C²H₂C³H₂ are almost the same as that of PMO-BINAPO. The chemical shift of C³ carbon species of Si–C¹H₂C²H₂C³H₂ appears at 47.5 ppm and is different from that of PMO-BINAPO (42.8 ppm), which further confirms the successful reduction of BINAPO to BINAP. The signal at 60.3 ppm is from the ethoxy groups. In addition, the new signal at 2.0 ppm can be ascribed to methyl group from the silylation process. ³¹P MAS NMR is a powerful technique to characterize the chemical state of phosphorus (Fig. 4). PMO-BINAPO shows a broad peak centered at about 29.7 ppm assigned to phosphorus of phosphine oxide in the ³¹P MAS NMR spectrum. For PMO-BINAP, the signal at –16.5 ppm which can be assigned to the reduced, unprotected phosphine shows the successful reduction of BINAPO to BINAP. The weak peak at 29.7 ppm is from some phosphine oxide buried in the pore wall which cannot be accessed by the reducing agent (HSiCl₃). The NMR results show the successful reduction of BINAPO to BINAP in the pore wall by post-synthesis modification method.

The FT-IR spectrum (Fig. 3) of PMO-BINAP shows the ureylene stretching vibration (1660 and 1537 cm⁻¹), P–C (aryl) vibration (1437 cm⁻¹), C–H (aryl) vibration (3057 cm⁻¹) and the

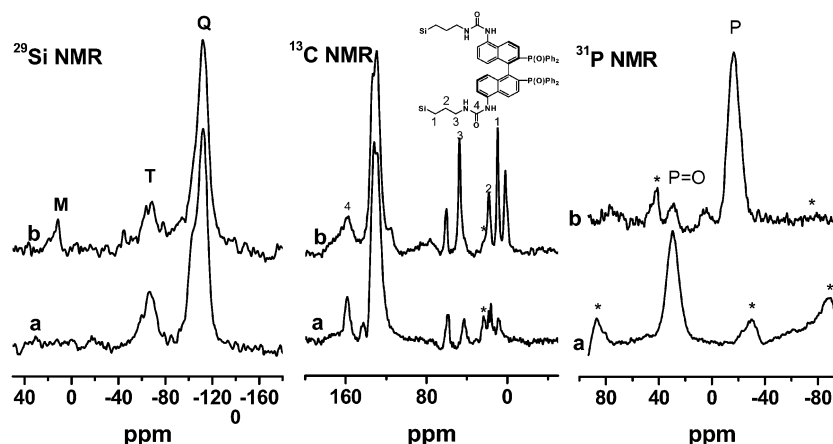


Fig. 4 Solid state ²⁹Si MAS (left), ¹³C CP MAS (middle) and ³¹P MAS (right) NMR spectra of PMO-BINAPO (a) and PMO-BINAP (b); *: side bands.

vibrations of propyl group (2900 cm^{-1}). In addition, the signal related with Si–H vibration is observed at around 2245 cm^{-1} ,³⁸ which shows the existence of trichlorosilane on the surface and in the pore channel of PMO-BINAP.

Ru/PMO-BINAP was synthesized by coordination of PMO-BINAP with $[\text{RuCl}_2(\text{benzene})]_2$ because the combination of Ru complex and BINAP could generate efficient catalyst for asymmetric hydrogenation. The Ru/P molar ratio in Ru/PMO-BINAP was $\sim 1/1.2$. For the homogeneous Ru/BINAP catalyst, the Ru/P molar ratio should be 1/2. The higher Ru/P molar ratio in Ru/PMO-BINAP is probably due to the fact the Ru complex can also react with surface hydroxyl group in the mesoporous channel in addition to coordination with BINAP.

The structural order of PMO-BINAP and Ru/PMO-BINAP was characterized by XRD and N_2 sorption isotherm and compared with that of PMO-BINAPO (after silylation) (Fig. 1). Compared with PMO-BINAPO, only one sharp diffraction peak was observed in the XRD pattern of PMO-BINAP (after silylation). The disappearance of (110) and (200) may be due to the reduced contrast between the pore and wall after silylation. PMO-BINAP displays a broad diffraction peak in its XRD pattern. It is interesting to mention that Ru/PMO-BINAP shows a sharp diffraction peak similar to PMO-BINAPO after silylation. Therefore, the broad diffraction peak of PMO-BINAP is not from the deterioration of the structural order. It is probably due to the decreased contraction between the pore and wall (the existence of Si–H species was observed in the FT-IR spectrum of PMO-BINAP). The TEM image of PMO-BINAP clearly shows hexagonal pore arrangement, further confirming that this sample still has ordered 2-D hexagonal mesostructure. The d spacings of the sample decrease in the order of PMO-BINAPO > PMO-BINAP > Ru/PMO-BINAP (Table 1), probably due to the framework contraction in each modification step (each modification step involves high temperature treatment).

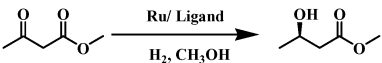
After silylanized with hexamethyldisilazane, PMO-BINAPO (after silylation) also shows type IV nitrogen sorption isotherm pattern with H1 hysteresis loop. After deoxidized with trichlorosilane, however, PMO-BINAP shows type IV nitrogen sorption isotherm pattern with H3 hysteresis loop. It is worthy to mention that Ru/PMO-BINAP shows a type IV nitrogen sorption isotherm pattern with an H1 hysteresis loop similar to PMO-BINAPO. Moreover, the pore volume and pore diameter of Ru/PMO-BINAP is greatly increased compared with that of PMO-BINAP. On passing from PMO-BINAP to Ru/PMO-BINAP, important changes of textural properties were observed. There are three reasons for the corresponding change. (1) Before reduction, PMO-BINAPO was silylanized with hexamethyldisilazane. In this process, a decreased surface area and pore diameter was observed. (2) During the reduction process of BINAPO into BINAP, some trichlorosilane was adsorbed onto the surface of the material (this was identified by FT-IR spectroscopy, Fig. 3c), which caused the further reduction of pore diameter and pore volume. (3) In the process of coordination of PMO-BINAP with $[\text{RuCl}_2(\text{benzene})]_2$, the adsorbed trichlorosilane was removed in the boiling ethanol solution. The vibrations related with Si–H cannot be observed at around 2245 cm^{-1} in the FT-IR spectrum of Ru/PMO-BINAP (Fig. 3d). Therefore, the surface area and pore diameter of Ru/PMO-BINAP was increased. Compared with the FT-IR spectrum of

Ru-BINAP (Fig. S1†), the vibration at 1382 cm^{-1} is probably from $[\text{RuCl}_2(\text{benzene})]_2$ and the vibration at around 1516 cm^{-1} indicates the successful coordination of $[\text{RuCl}_2(\text{benzene})]_2$ with BINAP (Fig. 3d). Above characterizations confirm that BINAP ligand in chiral PMO (PMO-BINAP) can coordinate with $[\text{RuCl}_2(\text{benzene})]_2$ for the formation of heterogeneous asymmetric catalyst.

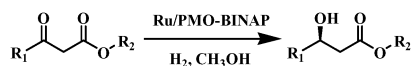
3.3. Catalytic performance of Ru/PMO-BINAP

The catalytic performance of Ru/PMO-BINAP was tested in the asymmetric hydrogenation of β -keto esters. As shown in Table 2, the metal complex, $[\text{RuCl}_2(\text{benzene})]_2$, shows a conversion of 13.9% in the hydrogenation of methyl acetoacetate and gives the racemic product. Ru/PMO-BINAP shows a complete conversion with 93.5% ee. Under similar conditions, the ee value obtained on homogeneous Ru/BINAP is 99%. The lower enantioselectivity of Ru/PMO-BINAP is probably due to the existence of uncoordinated $[\text{RuCl}_2(\text{benzene})]_2$ on chiral PMO (the molar ratio of Ru : P $\approx 1 : 1.2$). The conversion and ee do not change obviously with the S : C ratio varying from 100 to 1000. Even when the S : C ratio decreased to 2000, methyl acetoacetate could still be transformed into methyl-3-hydroxybutyrate with 91.0% conversion and 89.5% ee. Moreover, a number of different β -keto esters can be converted into the corresponding chiral alcohol on Ru/PMO-BINAP with S : C = 1000 (Table 3). The structures of the β -keto esters significantly affect the catalytic performance of Ru/PMO-BINAP. β -Keto esters bearing larger substituents in the R_2 position result in higher enantioselectivity than those bearing smaller one. For benzyl acetoacetate, the ee could reach as high as 99.0%. We also found that for methyl propionylacetate with proper steric hindrance of R_1 , the ee could reach as high as 99.1%. The above results suggest that Ru/PMO-BINAP is an efficient catalyst for asymmetric hydrogenation. The recycling ability of Ru/PMO-BINAP was primarily investigated in the hydrogenation of methyl acetoacetate. For the first cycle, complete conversion of the substrate with 90.4% ee was observed (Table 2). The slight decreasing of ee is probably due to the air-sensitivity of the catalytically active Ru-hydride species.^{33,36} The further recycling ability of the catalyst is under investigation.

Table 2 Asymmetric hydrogenation of methyl acetoacetate catalyzed by Ru/PMO-BINAP with various ratios of substrate to catalyst.^a

			
Catalyst	S : C	Conversion (%)	E.e. (%)
$[\text{RuCl}_2(\text{benzene})]_2$	1000	13.9	0
Ru/BINAP	1000	99.0	99.9
Ru/PMO-BINAP	100	99.0	94.2
Ru/PMO-BINAP	200	99.0	93.7
Ru/PMO-BINAP	500	99.0	93.4
Ru/PMO-BINAP	1000	99.0 (99.0) ^b	93.5 (90.4) ^b
Ru/PMO-BINAP	2000	91.0	89.5

^a Conversions and ee values were determined by GC on a Supelco γ -DEX 225 capillary column. All the reactions were carried out under a hydrogen pressure of 4 MPa in 1.0 mL methanol at 50°C for 24 h. ^b The data in parentheses are the result of the first recycling.

Table 3 Asymmetric hydrogenation of β -keto esters catalyzed by Ru/PMO-BINAP.^a

R	Conversion (%)	E.e. (%)
R ₁ = Me, R ₂ = Et	99.0	92.2
R ₁ = Me, R ₂ = ⁱ Pr	99.0	92.5
R ₁ = Me, R ₂ = ^t Bu	99.0	95.1
R ₁ = Me, R ₂ = CH ₂ -Ph	99.0	99.0
R ₁ = Me, R ₂ = CH ₂ -CHCH ₃	99.0	93.2
R ₁ = Et, R ₂ = Me	99.0	99.1
R ₁ = ⁱ Pr, R ₂ = Me	99.0	93.2
R ₁ = 4'-OMe-Ph, R ₂ = Et	99.0	92.8

^a Conversions and ee values were determined by GC on a Supelco γ -DEX 225 capillary column. Unless otherwise specified, all the reactions were carried out under a hydrogen pressure of 4 MPa in 1.0 mL methanol at 50 °C for 24 h with S : C = 1000.

4. Conclusions

In summary, we have successfully incorporated air sensitive C₂-symmetric chiral building blocks, BINAP, in the pore wall of PMO by post-synthesis reduction of highly ordered PMO with BINAPO bridging chiral ligand which was synthesized by co-condensation method under hydrothermal conditions. The NMR results show the successful reduction of BINAPO to BINAP in the pore wall by post-synthesis modification method. No obvious deterioration of structural order was observed during the post-synthesis modification process. The chiral PMO has demonstrated excellent enantioselectivity (the highest ee up to 99%) in asymmetric hydrogenation of β -keto esters. The generality of this synthesis strategy should allow the synthesis of versatile high-performance chiral solids for a wide range of organic transformations.

Acknowledgements

This work was supported by the National Basic Research Program of China (2009CB623503), NSFC (20621063, 20673113) and Programme for Strategic Scientific Alliances between China and the Netherlands (2008DFB50130). We thank Prof. Yonggui Zhou for the useful discussions.

References

- 1 A. Corma, *Chem. Rev.*, 1997, **97**, 2373.
- 2 A. Stein, B. J. Melde and R. C. Schroden, *Adv. Mater.*, 2000, **12**, 1403.
- 3 M. Vallet-Regi, F. Balas and D. Arcos, *Angew. Chem., Int. Ed.*, 2007, **46**, 7548.

- 4 Y. Wan and D. Y. Zhao, *Chem. Rev.*, 2007, **107**, 2821.
- 5 M. E. Davis, *Nature*, 2002, **417**, 813.
- 6 F. Hoffmann, M. Cornelius, J. Morell and M. Froba, *Angew. Chem., Int. Ed.*, 2006, **45**, 3216.
- 7 T. Asefa, M. J. MacLachan, N. Coombs and G. A. Ozin, *Nature*, 1999, **402**, 867.
- 8 S. Inagaki, S. Guan, Y. Fukushima, T. Ohsuna and O. Terasaki, *J. Am. Chem. Soc.*, 1999, **121**, 9611.
- 9 B. J. Melde, B. T. Holland, C. F. Blanford and A. Stein, *Chem. Mater.*, 1999, **11**, 3302.
- 10 W. J. Hunkes and G. A. Ozin, *J. Mater. Chem.*, 2005, **15**, 3716.
- 11 M. P. Kapoor and S. Inagaki, *Bull. Chem. Soc. Jpn.*, 2006, **79**, 1463.
- 12 F. Hoffmann, M. Cornelius, J. Morell and M. Froba, *J. Nanosci. Nanotechnol.*, 2006, **6**, 265.
- 13 M. C. Burleigh, M. A. Markowitz, S. Jayasundera, M. S. Spector, C. W. Thomas and B. P. Gaber, *J. Phys. Chem. B*, 2003, **107**, 12628.
- 14 S. Shylesh, R. K. Jha and A. P. Singh, *Microporous Mesoporous Mater.*, 2006, **94**, 364.
- 15 E. B. Cho, K. W. Kwon and K. Char, *Chem. Mater.*, 2001, **13**, 3837.
- 16 W. P. Guo, X. Li and X. S. Zhao, *Microporous Mesoporous Mater.*, 2006, **93**, 285.
- 17 Q. H. Yang, J. Liu, L. Zhang and C. Li, *J. Mater. Chem.*, 2009, **19**, 1945.
- 18 F. Cozzi, *Adv. Synth. Catal.*, 2006, **348**, 1367.
- 19 Z. Wang, G. Chen and K. L. Ding, *Chem. Rev.*, 2009, **109**, 322.
- 20 K. Ding and Y. Uozumi, *Handbook of Asymmetric Heterogeneous Catalysis*. WILEY-VCH Verlag GmbH & Co. KGaA, Weinheim, 2008, pp. 1–24.
- 21 G. Ertl, H. Knözinger, F. Schüth and J. Weitkamp, *Handbook of Heterogeneous Catalysis*. 2 edn, Wiley-VCH Verlag GmbH & Co. KGaA, Weinheim, 2008, vol. 8, pp. 1–56.
- 22 C. Baleizao, B. Gigante, D. Das, M. Alvaro, H. Garcia and A. Corma, *Chem. Commun.*, 2003, 1860.
- 23 C. Baleizao, B. Gigante, D. Das, M. Alvaro, H. Garcia and A. Corma, *J. Catal.*, 2004, **223**, 106.
- 24 M. Alvaro, M. Benitez, D. Das, B. Ferrer and H. Garcia, *Chem. Mater.*, 2004, **16**, 2222.
- 25 M. Benitez, G. Bringmann, M. Dreyer, H. Garcia, H. Ihmels, M. Waidelich and K. Wissel, *J. Org. Chem.*, 2005, **70**, 2315.
- 26 D. M. Jiang, Q. H. Yang, H. Wang, G. R. Zhu, J. Yang and C. Li, *J. Catal.*, 2006, **239**, 65.
- 27 R. Noyori and H. Takaya, *Acc. Chem. Res.*, 1990, **23**, 345.
- 28 R. Noyori, *Angew. Chem., Int. Ed.*, 2002, **41**, 2008.
- 29 D. J. Bayston, J. L. Fraser, M. R. Ashton, A. D. Baxter, M. E. C. Polywka and E. Moses, *J. Org. Chem.*, 1998, **63**, 3137.
- 30 C. Chapuis, M. Barthe and J. Y. D. Laumer, *Helv. Chim. Acta*, 2001, **84**, 230.
- 31 S. Shimazu, K. Ro, T. Sento, N. Ichikuni and T. Uematsu, *J. Mol. Catal. A: Chem.*, 1996, **107**, 297.
- 32 T. Sento, S. Shimazu, N. Ichikuni and T. Uematsu, *J. Mol. Catal. A: Chem.*, 1999, **137**, 263.
- 33 A. G. Hu, H. L. Ngo and W. B. Lin, *J. Am. Chem. Soc.*, 2003, **125**, 11490.
- 34 A. G. Hu, H. L. Ngo and W. B. Lin, *Angew. Chem., Int. Ed.*, 2003, **42**, 6000.
- 35 A. G. Hu, G. T. Yee and W. B. Lin, *J. Am. Chem. Soc.*, 2005, **127**, 12486.
- 36 A. R. McDonald, C. Muller, D. Vogt, G. P. M. van Klinka and G. van Koten, *Green Chem.*, 2008, **10**, 424.
- 37 O. Muth, C. Schellbach and M. Froba, *Chem. Commun.*, 2001, 2032.
- 38 A. Mehdi and P. H. Mutin, *J. Mater. Chem.*, 2006, **16**, 1606.